Figure S1. Per-sample single-cell UMAP embeddings. UMAP plots displayed separately for the control (n=3) and bleomycin-model (n=3) groups. UMAP, Uniform Manifold Approximation and Projection.

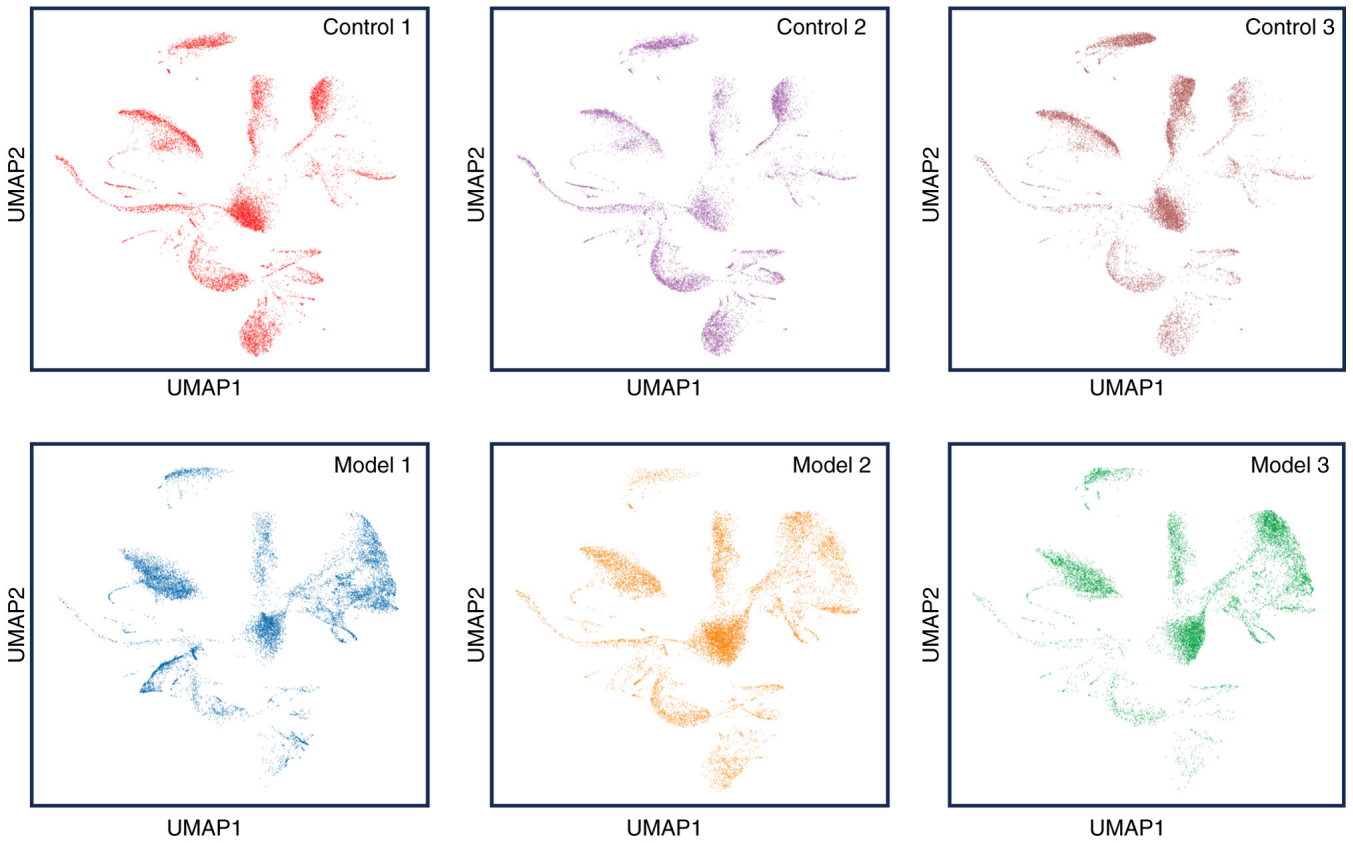

Figure S2. Annotation of major cell types from single-cell RNA sequencing. Heatmap showing the expression of canonical marker genes used to identify and annotate the 10 major cell types within the integrated lung single-cell dataset.

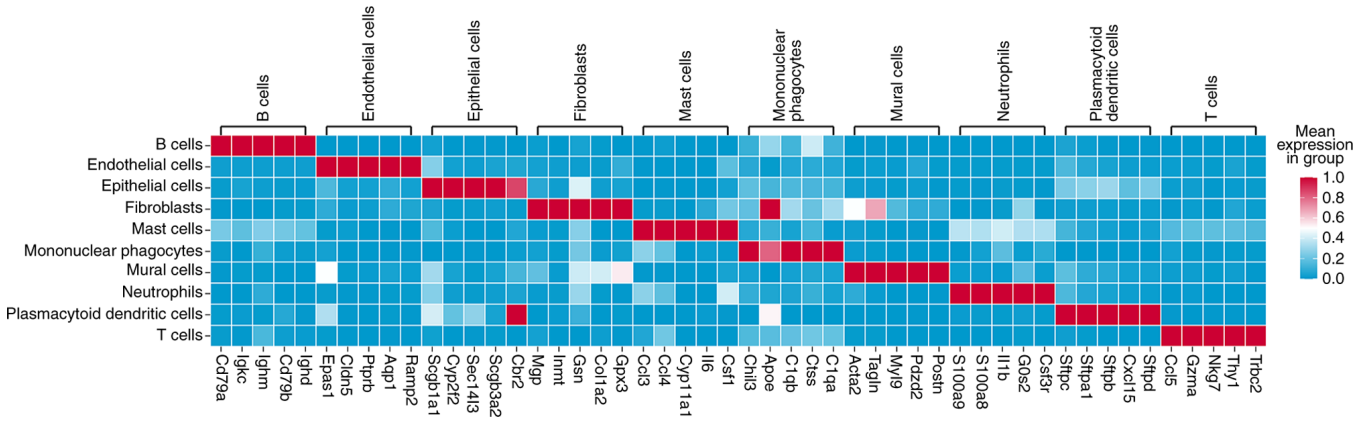

Figure S3. The molecular size of HA after sonication was assessed by agarose gel electrophoresis. HA, hyaluronic acid.

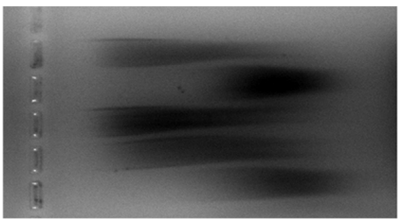

Figure S4. Dynamic hydrogen bonding profile between OG and HAS2 from MDS. OG, glucoside; HAS2, hyaluronic acid synthase 2; MDS, molecular dynamics simulation.

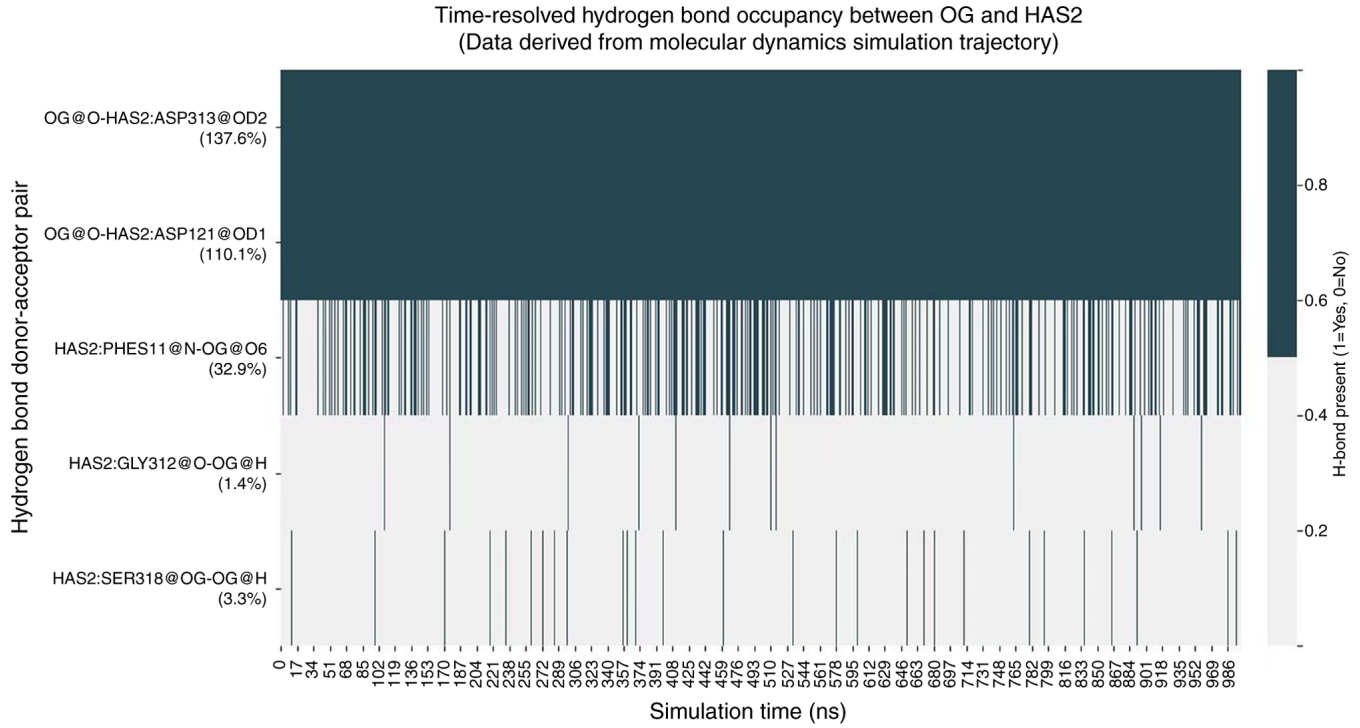

Figure S5. HA and IL-4/IL-13 cytokine synergy in macrophage M2 polarization. RAW264.7 macrophages were treated with HA (50 μg/ml), IL-4 plus IL-13 (both at 20 ng/ml), or a combination of both for 24 h. TGF-β1 concentration in the culture supernatant was quantified by ELISA. HA, hyaluronic acid.

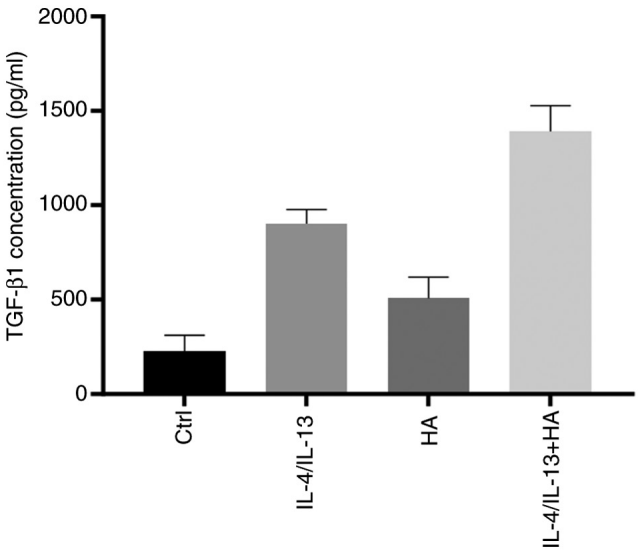

Figure S6. Computational assessment of OG binding affinity across HAS isoforms. Molecular docking was performed to predict the binding energy of OG with HAS1, HAS2, and HAS3 protein structures. OG, glucoside; HAS, hyaluronic acid synthase.

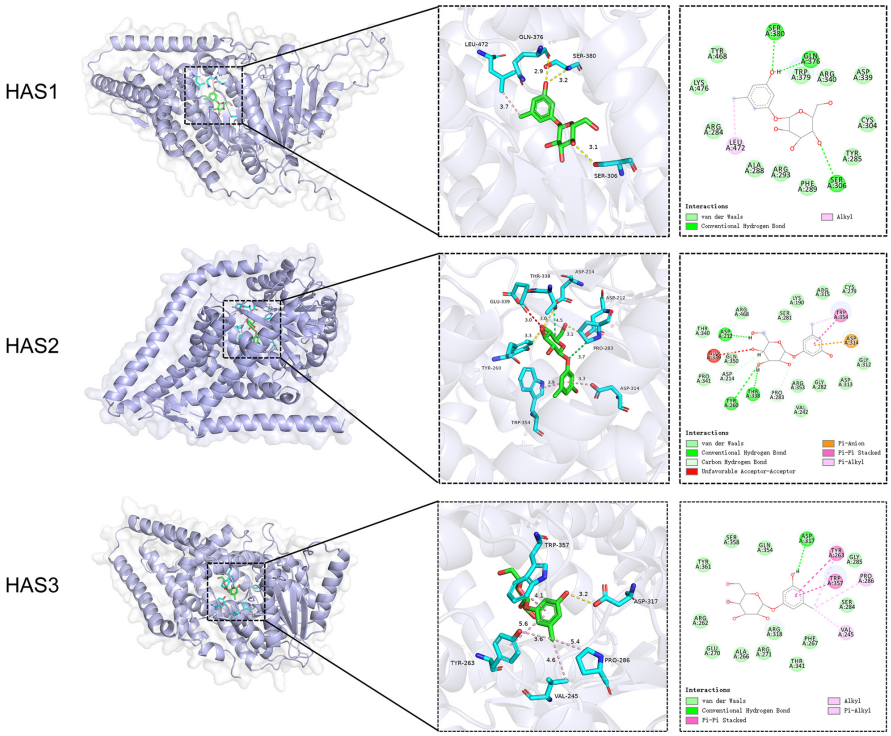

protein	binding energy (kcal/mol)
HAS1	6.715
HAS2	–7.777
HAS3	–6.486